# STAR FORMATION TRIGGERING BY DENSITY WAVES IN THE GRAND DESIGN SPIRALS NGC 3992 AND NGC 628

JORDI CEPA
Instituto de Astrofísica de Canarias; and La Palma Observatory, Tenerife, Spain

AND

JOHN E. BECKMAN
Instituto de Astrofísica de Canarias, Tenerife, Spain
*Received 1989 March 27; accepted 1989 July 1*

## ABSTRACT

Although spiral structure in grand design galaxies is generally present in the young and old stellar components and also in both atomic and molecular gas, the issue of whether the spiral structure is merely "organized" by a density wave, or whether star formation is triggered preferentially in the arms is still an open question. Here we present evidence which appears to favor triggering, or more correctly nonlinear dependence of star formation efficiency on the underlying gas density. Starting with a detailed Hα map of NGC 3992, a well-ordered four-armed spiral, of type 9 on Elmegreen's scale (where 1 is flocculent and 12 highly ordered), we define an efficiency index for massive star formation based on the ratio of the density of ionizing photons from these stars to the underlying H I density. We show that the arm/interarm ratio of this index, on length scales of $\sim 1$ kpc, which would take values close to unity if star formation rate depend linearly on the H I density, rises to values of well over 10, peaking at $\sim 25$, which each arm showing comparable behavior. There is, in addition, a striking dip to unity in the ratio, for all arms, at a common galactocentric radius, which we suggest is that of corotation. The arm class 9 galaxy NGC 628 shows highly comparable behavior. Given that star formation rates almost certainly depend on $H_2$ and not H I densities, that recent evidence for M51 (Vogel *et al.*) shows strong $H_2$ clumping in the arms, but that *average* arm/interarm $H_2$ densities are generally not greater than $\sim 3$, on scales of 1 kpc, and shown no significant changes at corotation, the present evidence points to a nonlinear star formation rate enhancement mechanism, functioning via preferential formation of dense $H_2$ clouds in arms, at sites other than the corotation and the Lindblad resonance radii. The observed absence of high arm/interarm ratios of the efficiency index in the flocculent galaxy M33 tends to confirm this reasoning.

*Subject headings:* galaxies: individual (NGC 628, 3992) — galaxies: stellar content — galaxies: structure — stars: formation

## I. INTRODUCTION AND OBSERVATIONS

We describe the results of observations designed to investigate, on kiloparsec scales, the dependence of the star formation efficiency in spirals on the underlying gas density. The question addressed here is normally referred to as that of triggering. It is widely accepted that the surface densities of the gas (Visser 1978) and of the older disk stars (Elmegreen and Elmegreen 1984) in well-ordered spirals are modulated by a spiral density wave (hereafter SDW; see Lindblad 1950; Lin 1968) as measured in 21 cm emission from H I and in smoothly modulated IR emission for the stellar components, respectively. It is less clear, however, whether the enhanced star formation rate in spiral arms is due essentially to the enhanced gas densities "organized" in the arms by the SDW or whether there is in addition specific triggering, perhaps associated with the supersonic propagation of the density wave through the gas. In the present empirical study we do not aim to explain the results via any specific triggering mechanism or scenario, because as explained below, further important observations are still required to complete the physical picture. We will claim, however, that the observations reported here place important and striking constraints on models.

The spirals used in this work are NGC 628 for which all the data, both in Hα and H I 21 cm, were taken from the literature (Hodge 1976; Kennicutt and Hodge 1980, for the Hα data, and

Wevers 1984 for the 21 cm neutral hydrogen distribution and rotation curve), and NGC 3992, for which we obtained images in Hα with the TAURUS camera at the cassegrain focus of the 4.2 m William Herschel Telescope at the Roque de Los Muchachos Observatory, La Palma. The large galaxy diameter required a mosaic map in nine fields, each composed of two 10 minute exposures in Hα and a 5 minute broad-band exposure in the neighboring continuum, to subtract the stellar component of luminosity within the Hα filter. Angular resolution was, without autoguiding, 1″ over the field, corresponding to 69 pc at the distance of 14.2 Mpc to NGC 3992 (de Vaucouleurs 1979).

For NGC 3992 we assigned 392 distinct H II regions either to an arm or the interarm disc (Cepa and Beckman 1989), by comparison with the Palomar Sky Survey photograph, where four arms are distinguishable. There is little scope for confusion here; we estimate a maximum of 21 doubtful assignments. Figure 1 (Plate 3) shows the observations in direct image form, and Figure 2 is a diagram of our assignments.

## II. METHOD

Comparing the star formation *rates* (SFR) in the arm and interarm regions, would not necessarily offer useful information about triggering by an SDW, because a high SFR in an arm might simply be a function of an average higher gas
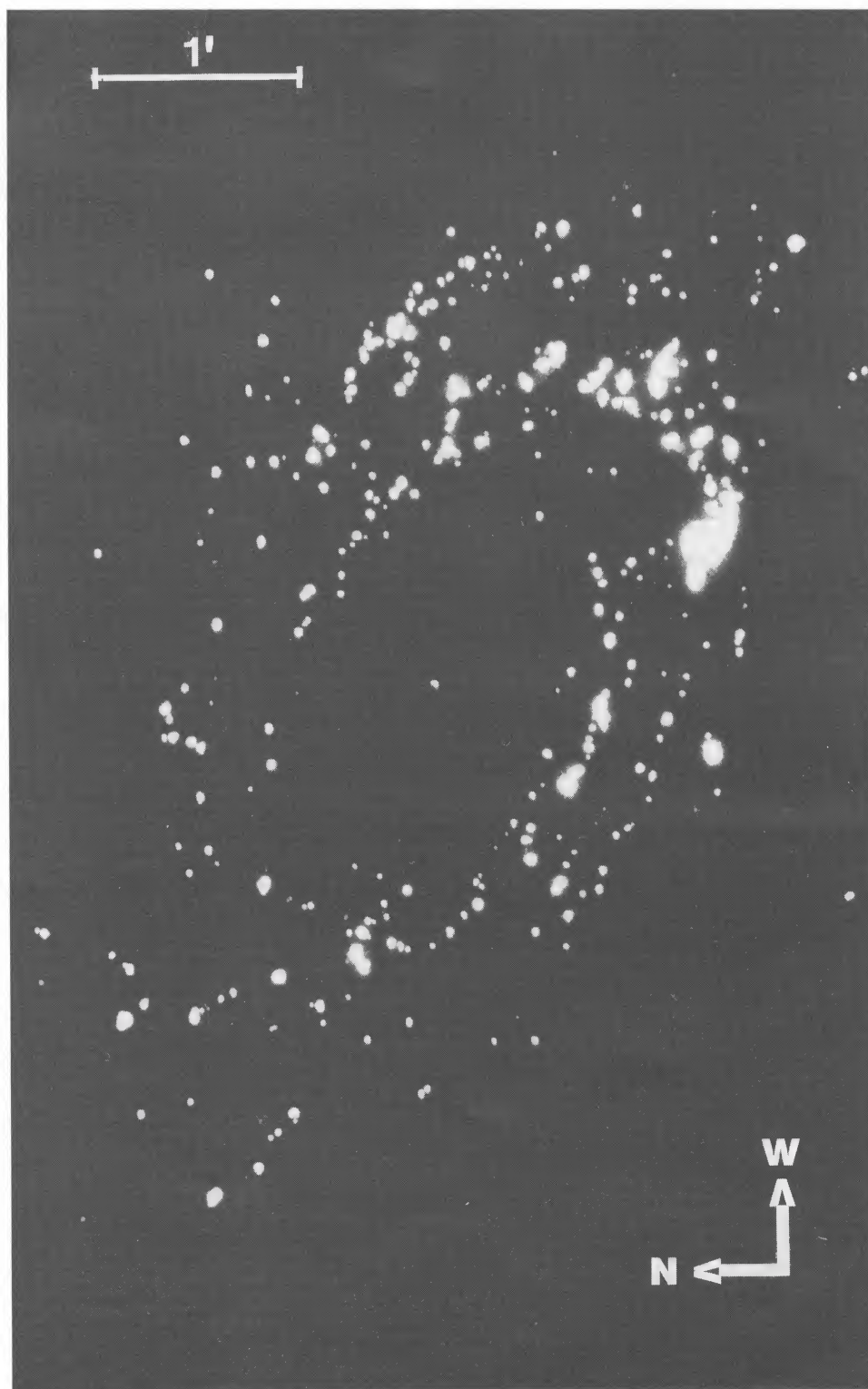
PLATE 3

FIG. 1.—Nine-frame mosaic of Hα minus continuum of NGC 3992, showing the 392 H II regions detected. The point at the center does not correspond to an H II region, but is the residual of the nucleus after continuum subtraction.
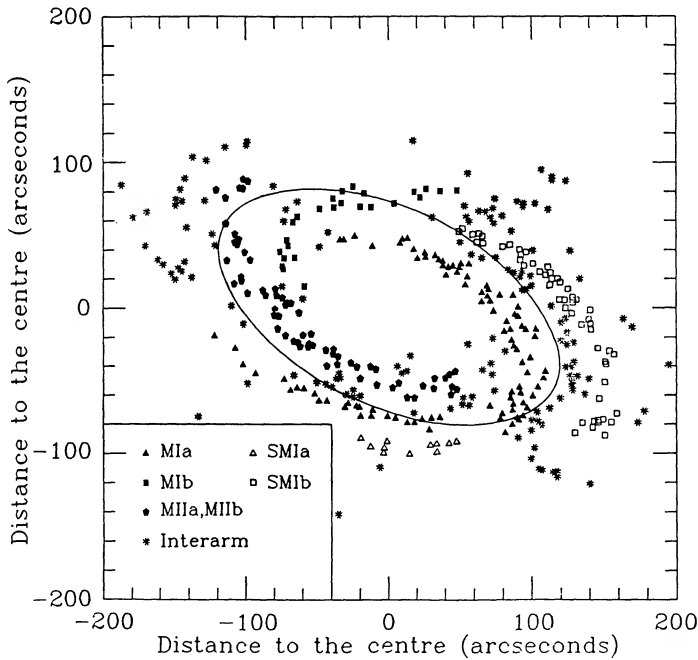
CEPA AND BECKMAN (see **349**, 497)

FIG. 2.—Diagram of assignments of the H II regions of NGC 3992. Each point style corresponds to a different assignment either to a spiral arm or to the interarm region as shown in the key. The ellipse marks the zone where the arms show discontinuities and splittings.

density there. We therefore make an arm-interarm comparison of the massive star formation *efficiency* which we may define as the mass of young stars per unit area of disk surface divided by the surface density of neutral gas at the same position. We could predict that if the ratios of arm to interarm star formation efficiency were much greater than unity, this would be *prima facie* evidence that some nonlinear mechanism is at work which, by detailed measurement, could be elucidated in physical terms.

Our star forming efficiency index $\epsilon$ is defined in terms of the radii $r_i$ of the H II regions within a star-forming region, from our CCD exposure, and the column densities $\sigma_i$ of neutral atomic hydrogen H I, obtained in the case of NGC 3992 from the 21 cm map of Gottesman *et al.* (1984). The basic physics is that of the Strömgren sphere around an ionizing star, with volume $V$ given by (Spitzer 1968):

$$V \propto \frac{S_{UV}}{n_H^2} \qquad (2.1)$$

where $S_{UV}$ is the number of UV photons emitted by the star at wavelengths shortward of the Lyman limit, and $n_H^2$ is the mean total (neutral and ionized) hydrogen density of the region, assuming each available photon ionizes a hydrogen atom. The technique is preferable to a simple integration of H$\alpha$ surface flux because the volume of an H II region is less affected by continuum subtraction uncertainties. We initially assume an invariant initial mass function (IMF) of star formation, and call $K^j$ the ratio of the number of UV photons to mass of ionizing stars in a given star-forming region $j$ with $n^j$ H II regions in it; this is a global mean luminosity to mass ratio for the region and not for any particular star within it. To quantify the volumes of the H II regions, we approximate any H II region $i$ in star-forming zones $j$ to a sphere of radius $r_i^j$, and normalize in units of a minimum radius $R$, assumed invariant. A term of form $\sum_{i=1}^{n^j} (r_i^j/R)^3$ represents a number of normalized

H II regions, each containing an equal mass of ionizing stars, provided the IMF and $n_H$ do not vary from region to region (we will consider the impact of variation in these parameters briefly below). Dividing this number by the total surface area $S^j$ of the star-forming zone gives a normalized "column density" of H II regions, and dividing this quotient by the averaged H I surface density $(\sum_{i=1}^{n^j} \sigma_i^j)/n^j$ gives the massive star formation efficiency (MSFE):

$$MSFE^j = \frac{\kappa^j}{S^j} \frac{n^j}{\sum_{i=1}^{n^j} \sigma_i^j} \sum_{i=1}^{n^j} \left(\frac{r_i^j}{R}\right)^3, \qquad (2.2)$$

where

$$\kappa^j = C\left(\frac{\langle n_H^2 \rangle^j}{K^j}\right), \qquad (2.3)$$

where $C$ is a constant.

The use of equation (2.2) offers a direct, and observationally straightforward way to define an index of star formation efficiency. However, if we had preferred to define it in terms of the mass of stars in a given star-forming zone divided by a total initial mass available prior to the onset of star formation, we would have needed to supplement the denominator by three terms, one representing the mass contained in the stars themselves, the second representing the mass of ionized gas in the H II regions, and the third the mass of molecular gas. The denominator of (2.2) would then read:

$$\sigma_i^j = \sigma_i^j(\text{H I}) + \sigma_i^j(*) + \sigma_i^j(\text{H}^+) + \sigma_i^j(\text{H}_2), \qquad (2.4)$$

where the respective terms refer to equivalent column densities in H I, stars, H$^+$ and H$_2$, obtained by dividing the total mass of each component in a star-forming zone by the area of the zone. Although the additional terms differ in the facility with which they can be reliably evaluated, we can show, by estimating them, that their inclusion would not significantly change our results. Considering a star-forming zone, which in NGC 3992 and NGC 628 has a typical diameter somewhat greater than 1 kpc (so we take 1 kpc as a conservative estimate), the mass of H I in the zone is $2 \times 10^6$ $M_\odot$, using a conservative column density of $5 \times 10^{20}$ cm$^{-2}$ (Wevers 1984). The mass of newly formed stars can be conservatively inferred from our H$\alpha$ data at $10^3$–$10^4$ $M_\odot$, which clearly cannot contribute a significant effective column density to the denominator of (2.4). The contribution of ionized gas is more important. If we consider our giant H II complexes to have diameters of 100 pc, and mean densities of 10 cm$^{-3}$, and we take a value of five regions per star-forming zone (which is higher than the means for NGC 3992 and NGC 628), this gives $3.5 \times 10^5$ $M_\odot$ in ionized gas. This is not a major fraction of the neutral H I, and in a hypothetical case where there were 3 times more H II regions in the arm than in an equivalent star-forming zone in the neighboring disk, would affect the resulting ratio of efficiency indices by no more than some 10%.

It is more difficult to account quantitatively for the molecular gas given the lack of H$_2$ (i.e., CO) maps of NGC 3992 and NGC 628 (and of galaxies in general) with arms detected and resolved. To weaken our eventual conclusion qualitatively, however, the arm/interarm contrast in H$_2$, averaged over scales of an arm width, i.e., $\sim 1$ kpc, would have to be consistently greater than 3, which for available one-dimensional profiles in CO (e.g., Tacconi 1988), does not appear to be the case. The most detailed CO maps so far presented, those of M51 (Vogel, Kulkarni, and Scoville, 1988) show that the averaged CO arm/interarm contrast on scales of the order of 500 pc is of

order 3; which is entirely in agreement with our assumption because this spatial resolution is comparable to that of our star-forming zones (see Fig. 3, text below, and Braunsfurth and Feitzinger 1985 and references therein) which have characteristic scales larger than 1 kpc. Moreover, $H_2/H$ I surface density ratios appear to fade quite rapidly at values of galactocentric radius well within the scope of the present study. If we attempt a "rule of thumb" numerical approach, and attribute some $10^5$ $M_\odot$ of molecular gas per H II region, this would produce a total contribution to the star forming zone of $5 \times 10^5$ $M_\odot$ in molecules. Even an overall arm/interarm density contrast of 10 in purely molecular gas which is, as we have explained above, higher than expected, would change the efficiency ratio, arm/interarm, by only some 25%. Thus our index is quite stable against all probable changes in the additional terms of (2.4).

Our test for triggering in the arms consists in plotting the ratio $\epsilon \equiv MSFE_{arm}/MSFE_{interarm}$ as a function of galactocentric radius. We can take a conservative approach to the ratio $\kappa_{arm}/\kappa_{interarm}$ by expressing it as

$$\frac{\kappa_{arm}}{\kappa_{interarm}} = \frac{K^{interarm}}{K_{arm}} \frac{\langle n_H^2 \rangle^{arm}}{\langle n_H^2 \rangle^{interarm}} . \quad (2.5)$$

If the IMF were the same in the arms and interarm zones, the ratio of the $K$'s would be unity, but taking a model with the arm IMF shifted to higher masses, e.g., that of Gusten and Mezger (1982), the ratio can fall to $\sim 0.6$. However, the value of the $\langle n_H^2 \rangle$ ratio will be typically of order 3 or more (Downes 1985). Thus, in general

$$\left( \frac{\kappa_{arm}}{\kappa_{interarm}} \right) \geq 1 , \quad (2.6)$$

and if we take it as unity, this gives a conservatively low estimate for $\epsilon$. We further note that our method is not affected by radial changes in the IMF (Terlevich and Melnick 1983; Terlevich 1985) due to galactic metallicity gradients.

If self-propagating star formation were the only physical process which forms and maintains the spiral arms, a value of order unity would be expected for $\epsilon$ over all the galactocentric distances at which the spiral arms are observed. If a spiral density wave is enhancing star formation, $\epsilon$ could be well above unity, because the conditions which lead to star formation in the arms could be very different from those in the interarm disk. Moreover, the radial dependence has to be consistent with the predictions of the spiral density wave theory: density waves can exist only between the inner Lindblad and the outer Lindblad resonances (Wielen 1974; Athanassoula 1984, defined as the radius at which (Lin 1968):

$$\Omega \pm \kappa/m = \Omega_p , \quad (2.7)$$

where $\Omega$ is the angular velocity of the galaxy at radius $R$ as measured in its rotation curve, $\Omega_p$ is the pattern speed, the plus sign corresponds to the outer Lindblad and minus sign to inner Lindblad resonances, $m$ is the number of arms, and $\kappa$ is given by

$$\kappa^2 = (2\Omega)^2 \left( 1 + \frac{r}{2\Omega} \frac{d\Omega}{dr} \right) . \quad (2.8)$$

At a particular radius $r_c$, the corotation radius, the material of the disk, in its differential rotation, equals the pattern speed ($\Omega = \Omega_p$). If we consider the component of the difference between rotation speed and pattern speed projected perpen-
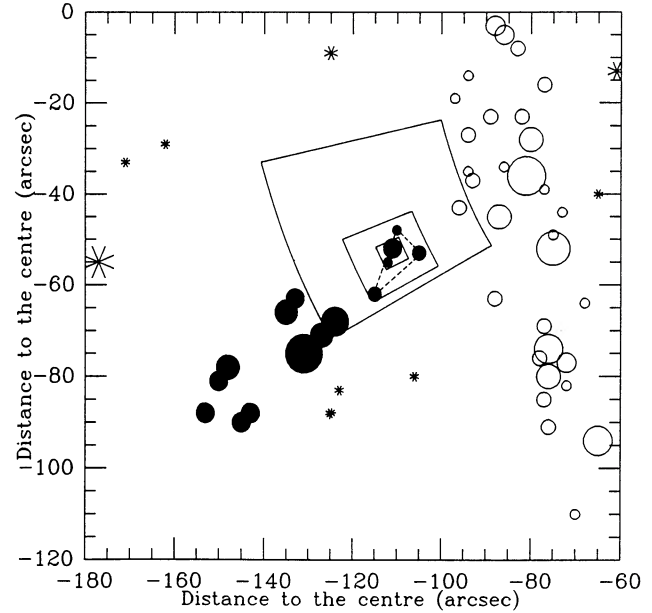


FIG. 3.—Idealized representation of a sector of the H II region distribution of the spiral NGC 628 taken from Hodge 1976 and Kennicutt and Hodge 1980, showing how we define and measure a typical star-forming zone. Each symbol style represents an H II region, the symbol diameter being proportional to the diameter of the region (assumed spherical). Empty circles correspond to H II regions classified by the authors as belonging to a given spiral arm, filled circles to H II regions belonging to another arm, and asterisks to interarm H II regions. Solid lines trace different trial cells, the outermost being too large because it includes H II regions belonging to different star-forming zones, the innermost being too small because only some of the H II regions of the star forming zone are included in it. The intermediate one represents the optimized cell size. The dashed line determines the area subtended by the star forming zone considered.

dicular to an arm of pitch angle $i$, the condition that a shock may be produced at a given radius $R$ is

$$|\Omega - \Omega_p| R \sin i > v_s , \quad (2.9)$$

where $v_s$ is the sound speed in the interstellar medium. As equation (2.9) cannot be satisfied at corotation, the gas at $r_c$ will not be shocked and $\epsilon$ would be of order unity, even in a scenario where shock-enhanced star formation does occur.

The effective column density of H II regions is computed via the number of H II regions per unit area of a star-forming zone, i.e., a zone where the H II regions are closely grouped. Star-forming zones can be located by finding regions with enhanced local density of H II regions per unit area. Their sizes are determined from the image of Figure 2 deprojected into the plane of the sky, dividing this image into annular sections of arc length equal to the radial annular width, as shown in Figure 3, and then adjusting the size of these cells at each point until the inferred column density of nonnormalized H II regions is a maximum within a given cell. This procedure allows us not only to determine the positions of the star-forming zones, their area and the number of H II regions in them, but also provides an estimate of the mean scale size of a typical zone, which is $1.7(\pm 0.5)$ kpc for NGC 3992 and $(870 \pm 390$ pc) for NGC 628, with no significant difference between the arms and the interarm disk in either galaxy. Measuring the MSFE's of the star-forming zones within a given annulus for each arm and for the interarm disk, we can derive $\epsilon$ as a function of radius.
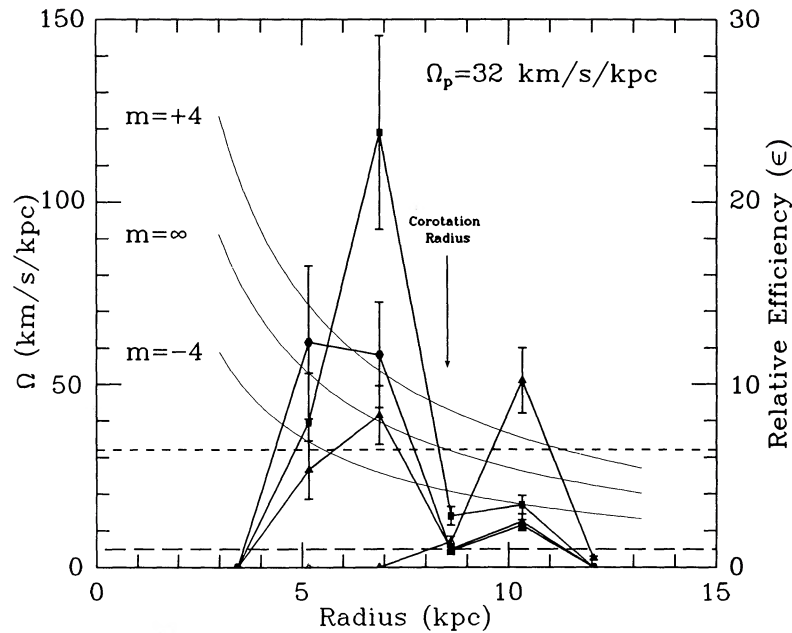
FIG. 4.—Relative arm/interarm star formation efficiency of NGC 3992 as a function of the galactocentric radius superposed on the diagram of velocities which shows the location of the inner and outer Lindblad resonances and the corotation radius for a four-armed spiral pattern, assuming a constant pattern speed of 32 km s$^{-1}$ kpc$^{-1}$ as a first approximation. The style of the symbols indicates the different arms according to the key of Fig. 2. The fine continuous curves represent $\Omega + \kappa/m$, with $\kappa$ defined in eq. (2.8). The short-dashed line shows $\Omega = \Omega_p$, and the long dashed line shows $\epsilon = 1$.

### III. RESULTS

In Figure 4 we plot $\epsilon$ against radius for the arms of NGC 3992, of arm class 9 (Elmegreen and Elmegreen 1987). We can see the striking results that in the region from 3.4 kpc to 12.0 kpc $\epsilon$ shows values consistently well above unity, rising to 10 or more in some places, but with a sharp dip to unity at 8.6 kpc. Not only do the excesses in $\epsilon$ imply some form of

nonlinear effect, but if we work with a constant pattern speed (of 32 km s$^{-1}$ kpc$^{-1}$), the minima in $\epsilon$ occur at values of $r$ consistent with corotation (9 kpc) and close to the inner and outer Lindblad resonances (6 kpc and 12 kpc, respectively) for a four-armed spiral (see Fig. 4). The position of the inner Lindblad resonance thus obtained is consistent, within our resolution limit, with the position of the end of the bar, con-
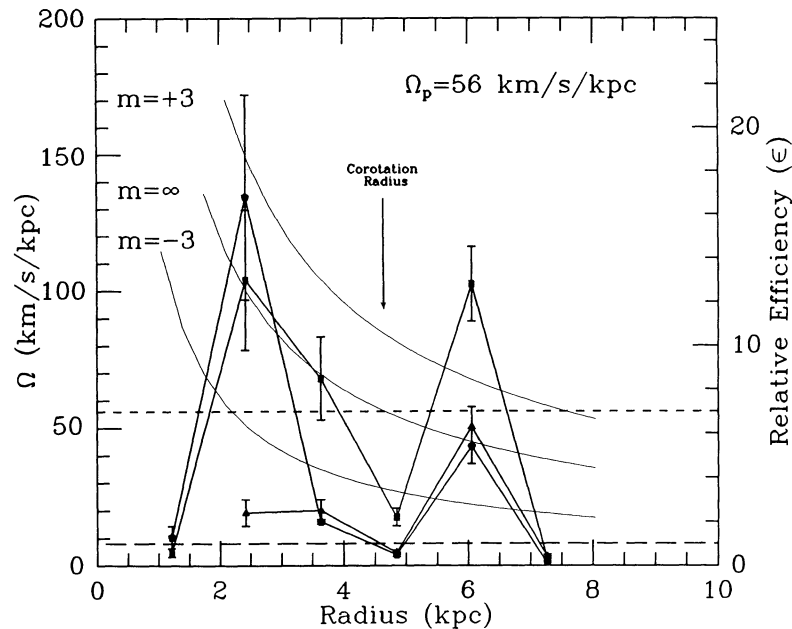


FIG. 5.—Relative arm/interarm star formation efficiency of NGC 628 as a function of the galactocentric radius superposed on the diagram of velocities which shows the location of the inner and outer Lindblad resonances and the corotation radius for a three-armed spiral pattern, assuming a constant pattern speed of 56 km s$^{-1}$ kpc$^{-1}$ as a first approximation. The style of the symbols indicates the different arms as classified by the authors. The fine continuous curves represent $\Omega + \kappa/m$, with $\kappa$ defined in eq. (2.8). The short-dashed line shows $\Omega = \Omega_p$, and the long-dashed line shows $\epsilon = 1$.
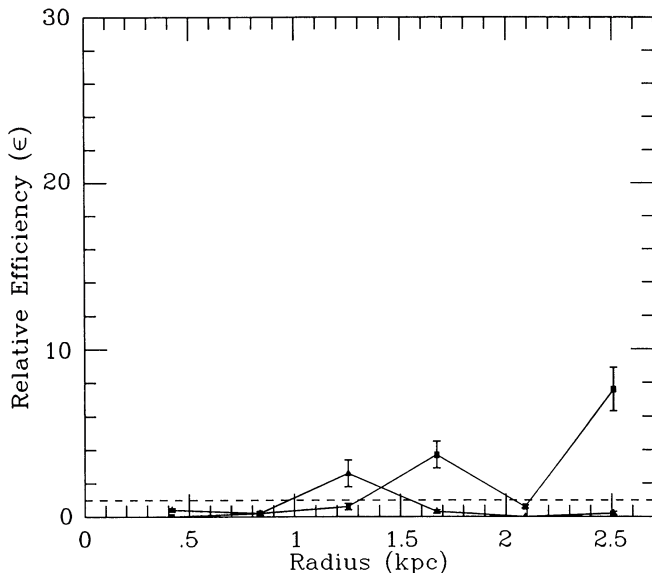
FIG. 6.—Relative arm/interarm star formation efficiency of M33 (NGC 598) as a function of the galactocentric radius. In this flocculent galaxy nonlinear effects of a spiral density wave are absent.

We may compare the results of the analysis for these two galaxies with those for the flocculent spiral M33: of arm type 5 (Elmegreen and Elmegreen 1987). Using data from Sabbadin, Rafanelli, and Bianchini (1980) for the H II regions, and an H I map of Newton (1980), $\epsilon$ as a function of radius was derived as plotted in Figure 6. The clear differences from Figures 4 and 5 are (a) lower values of $\epsilon$: less than 1 over most of the galaxy, and (b) no clear coincidences between the respective radii of maxima and minima in $\epsilon$ for the two arms. In fact the high value of $\epsilon$ in the outer part of one arm can be identified with a single "blob" of star formation, not reproduced elsewhere in the arms. We should note that although we have not shown, in the present paper, the detailed process of identification of the H II regions (as in Fig. 2 for NGC 3992) for those galaxies where the observational data were taken from the literature, in practice an entirely equivalent set of procedures was followed.

forming to predictions by various authors (see, e.g. Schempp 1982), and the enhanced values for $\epsilon$ occur over the same radial ranges for each arm. Moreover, (Fig. 2), this position for corotation coincides with the position of the splitting of the arm MIa, and the "break" in the arm MIb, features which are relatively common in spiral galaxies, and which could be explained as an effect of corotation (Saslaw 1985). It has often been proposed (see, for example, Feitzinger and Schmidt-Kaler 1980) that the spiral arms end at corotation, so the implications of Fig. 4 are clearly significant. We cannot exclude interpretations of our results in terms of other resonances and/or those induced by different standing modes, but if confirmed, we have a new approach to pattern speed determination.

As a more severe test of some form of triggering, we have repeated the procedure outlined here using the square of the H I column density and find qualitatively equivalent results, with numerical values consistent with those in Figure 4 within the error bars. We should also note that the H I column density itself (Gottesman et al. 1984) shows a smooth unpeaked continuous radial variation through corotation.

NGC 628, a three-armed spiral of arm class 9, appears to replicate NGC 3992 in all significant features, as shown in Fig. 5, including the similar dependence of the relative star-formation efficiency as a function of the radius for all the arms, and the pronounced minimum at corotation, working with a pattern speed of 56 km s$^{-1}$ kpc$^{-1}$. As in the case of NGC 3992, this position of corotation coincides with the zone where one arm splits, and another arm abruptly changes its pitch angle, as can be appreciated from the H$\alpha$ picture of Hodge (1980).

## IV. CONCLUSIONS

Although in this study we could not employ CO, and therefore $H_2$ surface densities, it is physically revealing, above all because of the geometrical behavior of the efficiency ratio: not only are there sharp dips in $\epsilon$ in all arms at corotation, but these do not correspond to any changes in the H I density. If $H_2$ is the true tracer of star formation (e.g., DeGioia-Eastwood et al. 1984), the very least that our study would predict is a sharp drop in the $H_2$/H I ratio at corotation in the arms, and this would be an important pointer to how the global star-forming process occurs in spirals. Given recent CO evidence (Vogel et al. 1988) that local $H_2$ cloud densities on scale lengths an order of magnitude smaller than those considered here may be much higher in the arms than in interarm regions, the present study can support the view that the route to massive star formation is via the agglomeration of small diffuse molecular clouds into denser giant clouds, either by collisions (Kwan and Valdes 1983; Roberts and Hausman 1984) or by gravitational instabilities (Elmegreen 1988). This agglomeration, at least, is directly triggered by the density wave. Until star formation theory or further observations, notably of $H_2$ give us the functional dependence of star formation rate on gas density, a study of the present global kind will not give a conclusive answer to the triggering problem. The results here do, however, show that the resonance effect in a spiral density wave plays a vital role in enhancing star formation in at least some grand design spirals, and we open up a possible new approach to pattern speed determination.

REFERENCES

Athanassoula, E. 1984, *Phys. Rept.*, **114**, 319.
Braunsfurth, E., and Feitzinger, J. V. 1985, *Astr. Ap.*, **144**, 215.
Cepa, J., and Beckman, J. 1989, *Astr. Ap. Suppl.*, **79**, 44.
DeGioia-Eastwood, K., Grasdalen, G. L., Strom, S. E., and Strom, K. M. 1984, *Ap. J.*, **278**, 564.
de Vaucouleurs, G. 1979, *Ap. J.*, **227**, 729.
Downes, D. 1985, *IAU Symposium 115*, ed M. Peimbert and J. Jugaku, 93.
Elmegreen, B. G. 1988, *Ap. J. (Letters)*, **342**, 67.

Elmegreen, D. M., and Elmegreen, B. G. 1984, *Ap. J. Suppl.*, **54**, 127.
———. 1987, *Ap. J.*, **314**, 3.
Feitzinger, J. V., and Schmidt-Kaler, Th. 1980, *Astr. Ap.*, **88**, 41.
Gottesman, S. T., Ball, R., Hunter, J. H., and Huntley, J. M. 1984, *Ap. J.*, **286**, 471.
Gusten, R., and Mezger, P. G. 1982, *Vistas Astr.*, **26**, 159.
Hodge, P. W. 1976, *Ap. J.*, **205**, 728.
Kennicutt, R. C., and Hodge, P. W. 1980, *Ap. J.*, **241**, 573.

Kwan, J., and Valdes, F. 1983, *Ap. J.*, **271**, 604.
Lin, C. C. 1968, In *Galactic Astronomy*, Vol. 2, ed. Hong-Yee Chiu and
    Amador Muriel (New York: Gordon & Breach).
Lindblad, B. 1950, *Stockholm Obs. Ann.*, **16**, No. 1.
Newton, K. 1980, *M.N.R.A.S.*, **190**, 689.
Roberts, W. W., and Hausman, M. A. 1984, *Ap. J.*, **277**, 744.
Sabbadin, F., Rafanelli, P., and Bianchini, A. 1980, *Astr. Ap. Suppl.*, **39**, 97.
Saslaw, W. C. 1985, *Gravitational Physics of Stellar and Galactic Systems*
    (Cambridge: Cambridge University Press).
Schempp, W. V. 1982, *Ap. J.*, **258**, 96.

Spitzer, L. 1968, *Diffuse Matter in Space* (New York: Wiley-Interscience).
Tacconi, L. J. Ph.D. thesis, University of Massachusetts (1988).
Terlevich, R. 1985, *Star Forming Dwarf Galaxies and Related Objects*, ed. D.
    Kunth, T. X. Thuan and Tran Thanh Van (Gil-sur-Yvette: Editions
    Frontières), p. 395.
Terlevich, R., and Melnick, J. 1983 ESO preprint, No. 264.
Visser, H. C. D. 1978, Ph.D. thesis, University of Groningen.
Vogel, S. N., Kulkarni, S. R., and Scoville, N. Z. 1988, *Nature*, **334**, 402.
Wevers, B. M. H. R. 1984, Ph.D. thesis, University of Groningen.
Wielen, R. 1974, *Pub. A.S.P.*, **86**, 341.

J. E. Beckman: Instituto de Astrofísica de Canarias, 38200 La Laguna, Tenerife, Spain

J. Cepa: Instituto de Astrofísica de Canarias, 38200 La Laguna, Tenerife, Spain